Supporting Information

Ultrathin nanosheet-assembled $[Ni_3(OH)_2(PTA)_2(H_2O)_4]\cdot 2H_2O$ hierarchical flowers for high-performance electrocatalysis of glucose oxidation reaction

*Shasha Zheng, Bing Li, Yijian Tang, Qing Li, Huaiguo Xue, Huan Pang**

School of Chemistry and Chemical Engineering, Guangling College

Yangzhou University, Yangzhou, 225009, Jiangsu, P. R. China.

E-mail: huanpangchem@hotmail.com; panghuan@yzu.edu.cn;

Homepage: http://huanpangchem.wix.com/advanced-material

Content

1. Materials

All chemicals, p-benzenedicarboxylic acid (PTA, 99%), $Ni(NO_3)_2 \cdot 6H_2O$, $Zn(NO_3)_2 \cdot 6H_2O$, N,N-dimethylformamide (DMF) and ethylene glycol, were purchased from Shanghai Sinopharm Chemical Reagent Co. and used without further purification. All aqueous solutions were freshly prepared with high purity water (18 MΩ cm).

2. Material characterization

The morphological features were characterized by field emission scanning electron microscopy (FESEM, Zeiss-Supra 55), high resolution transmission electron microscopy (HRTEM, Tecnai G2 F30 S-TWIN), and energy dispersive X-ray spectrometry (EDS) mapping. X-ray diffraction (XRD) patterns were examined on a Bruker D8 Advanced X-ray Diffractometer (Cu-Kα radiation: λ = 0.15406 nm). The chemical states were measured using an Axis Ultra X-ray photoelectron spectroscope (XPS, Kratos Analytical Ltd., UK) equipped with a standard monochromatic Al-Kα source (hv = 1486.6 eV). Fourier transform infrared (FTIR) transmission spectra were obtained on a BRUKER-EQUINOX-55 IR spectrophotometer. Inductively coupled plasma optical emission spectrometry (ICP-OES) analyses were carried out on a Perkin-Elmer Optima 7300DV spectrometer.

3. XRD patterns of P0-P6

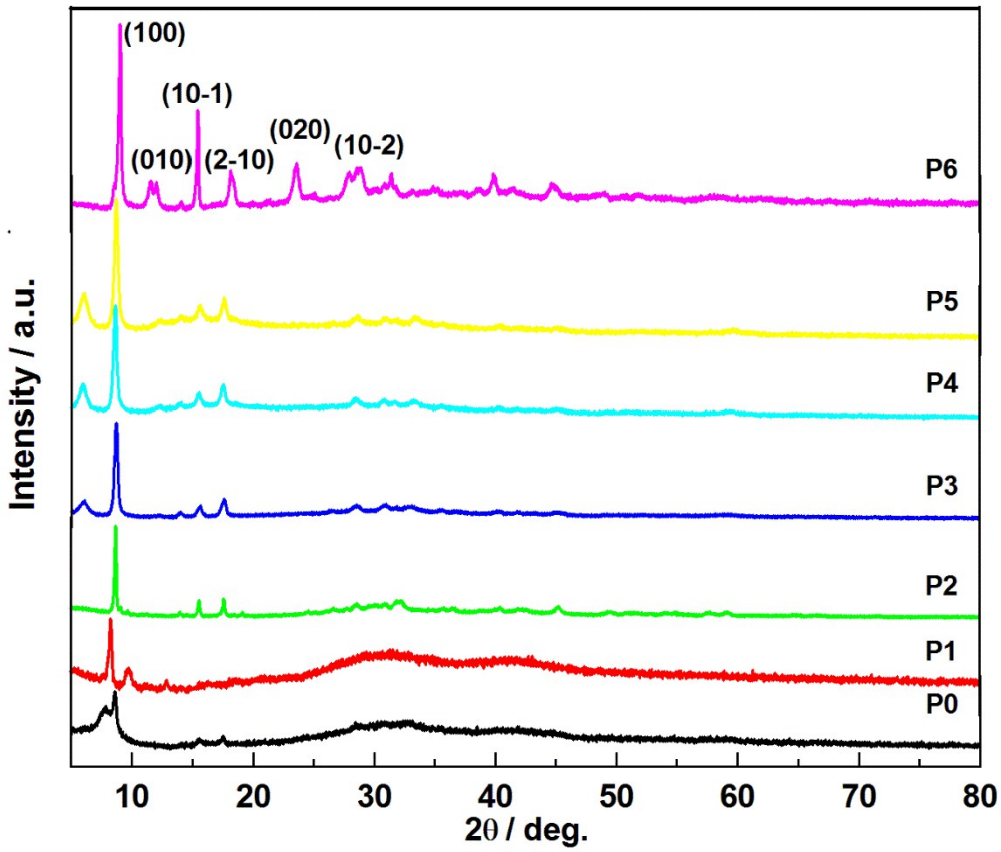

Figure S1. XRD patterns of P0-P6.

4. IR spectra of P0-P6

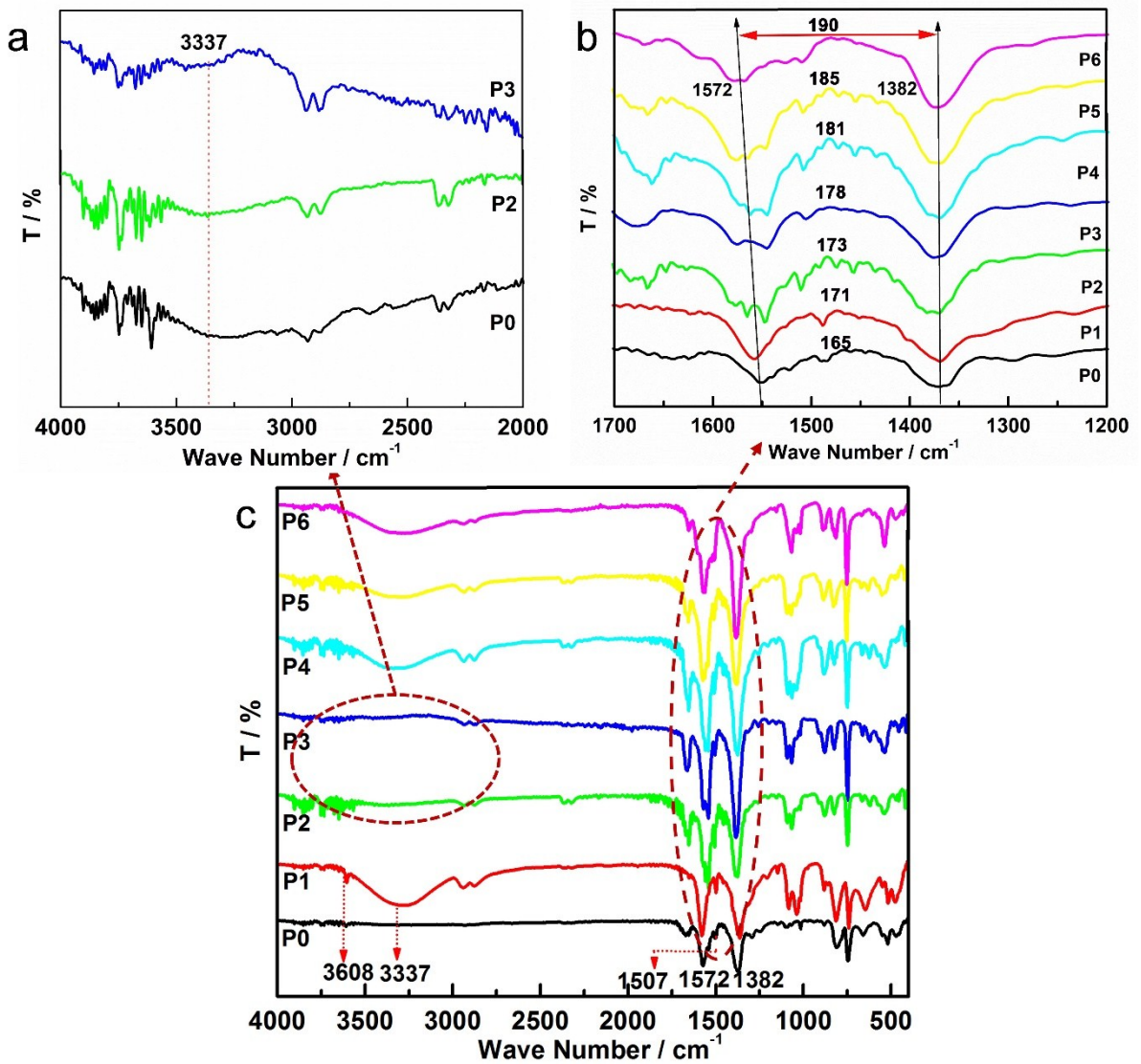

Figure S2. IR spectra of P0-P6.

5. SEM images of P0

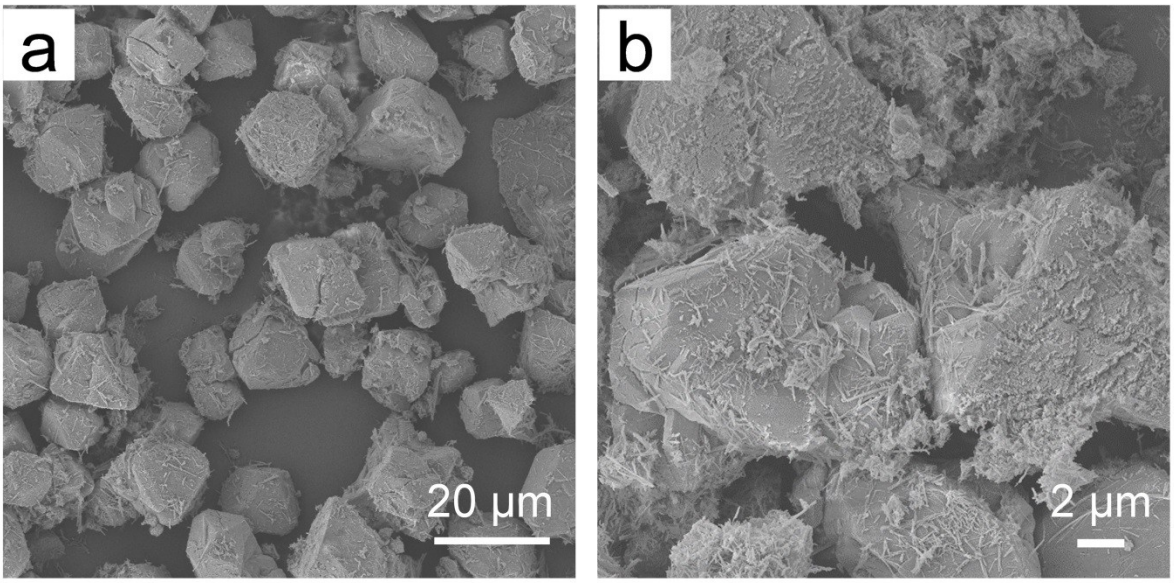

Figure S3. SEM images of: (a,b) P0.

6. TEM images of P1–P5

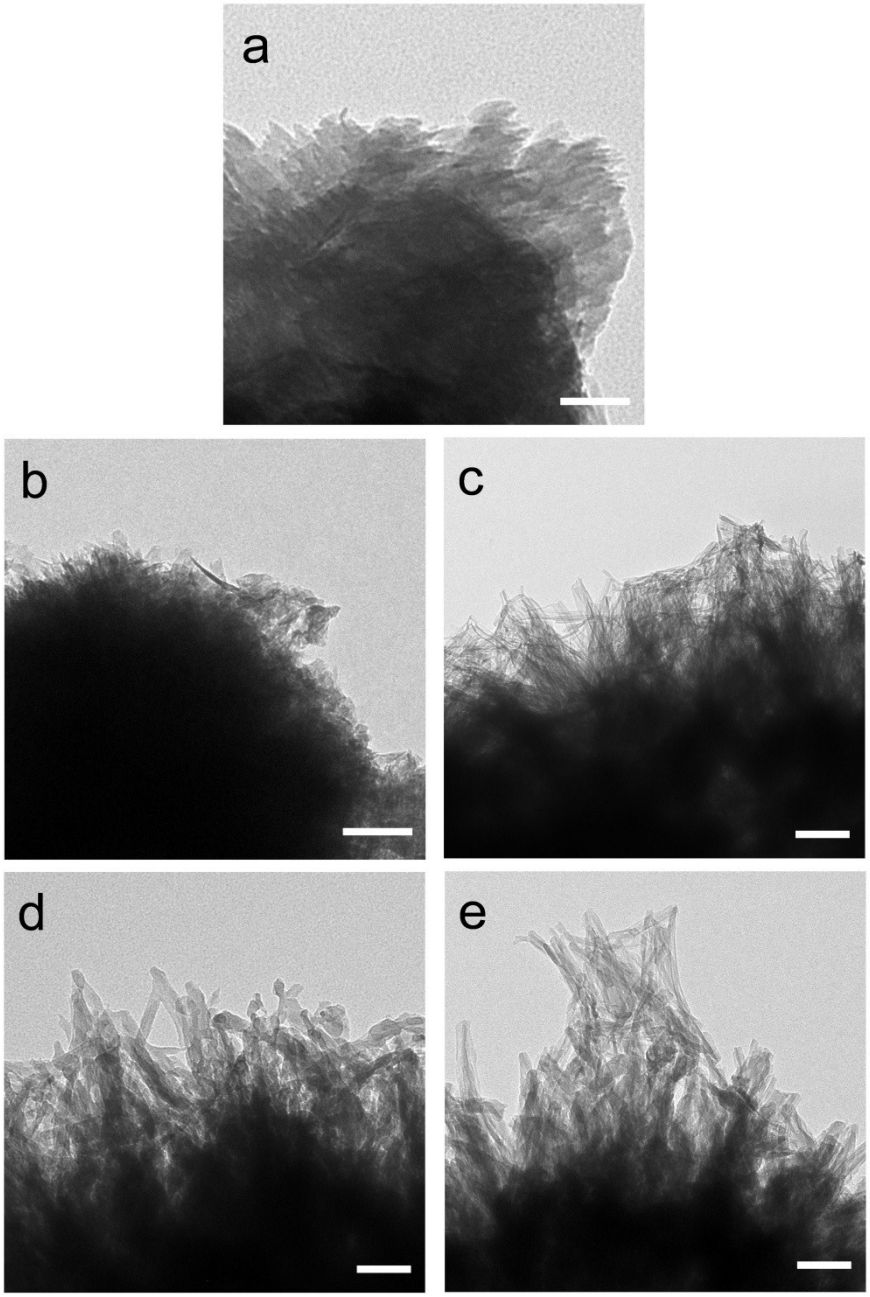

Figure S4. TEM (scale bar 100 nm) images of: (a) P1, (b) P2, (c) P3, (d) P4, (e) P5.

7. EDS analysis of P1-P5

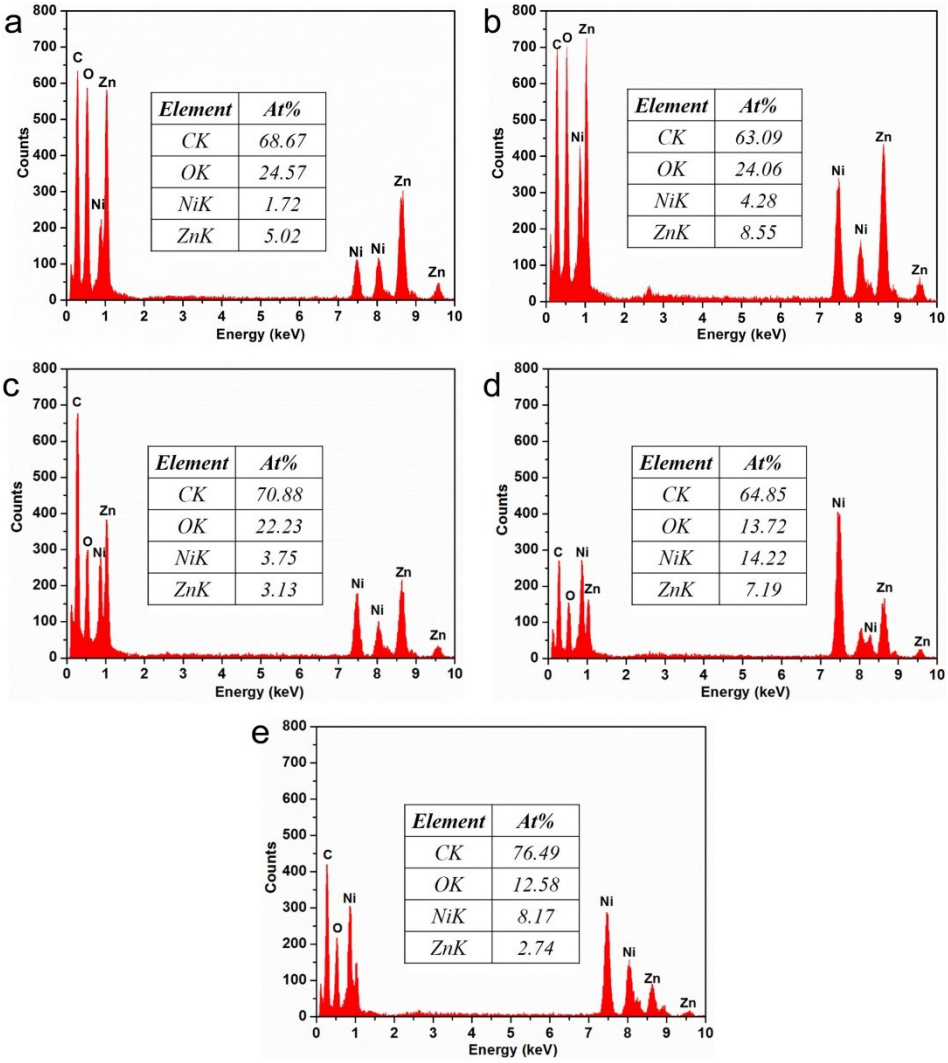

Figure S5. EDS analysis of: (a) P1, (b) P2, (c) P3, (d) P4, (e) P5.

8. Theoretical thickness of P6

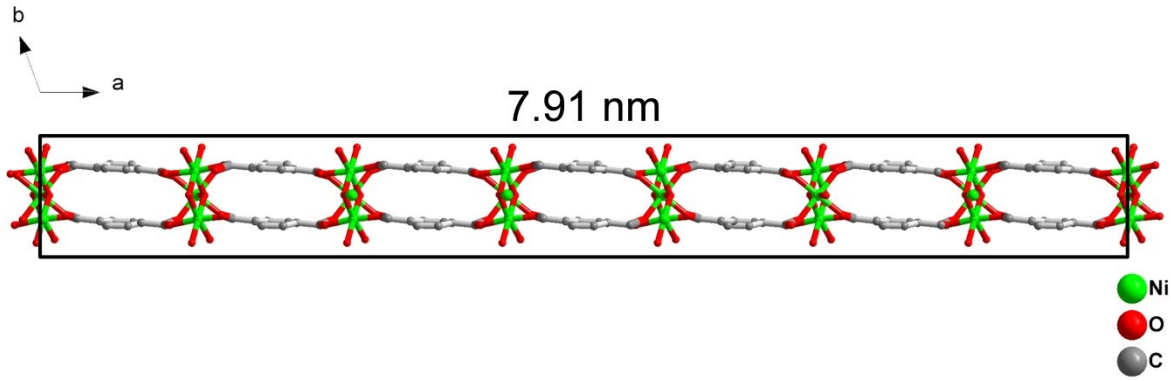

Figure S6. Theoretical thickness of P6 with eight metal coordination layers.

9. Ni 2p XPS analysis of P0-P6

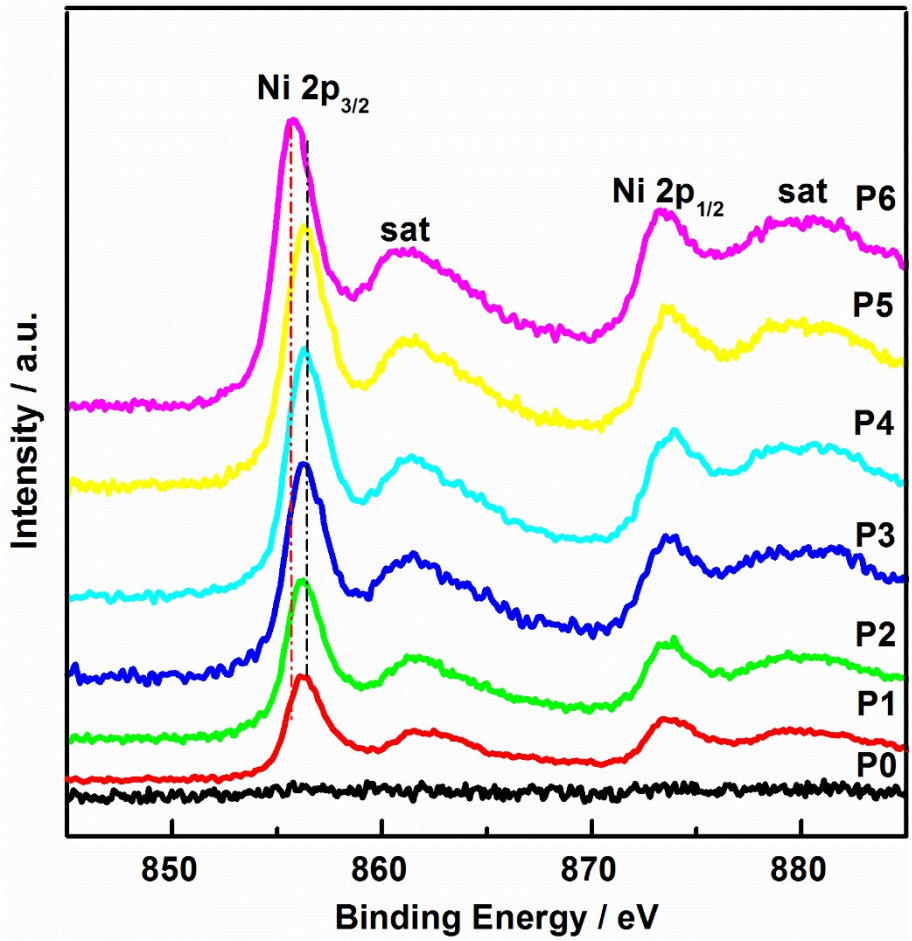

Figure S7. Ni 2p XPS spectra of the P0-P6 sample.

10. Zn 2p XPS analysis of P0-P6

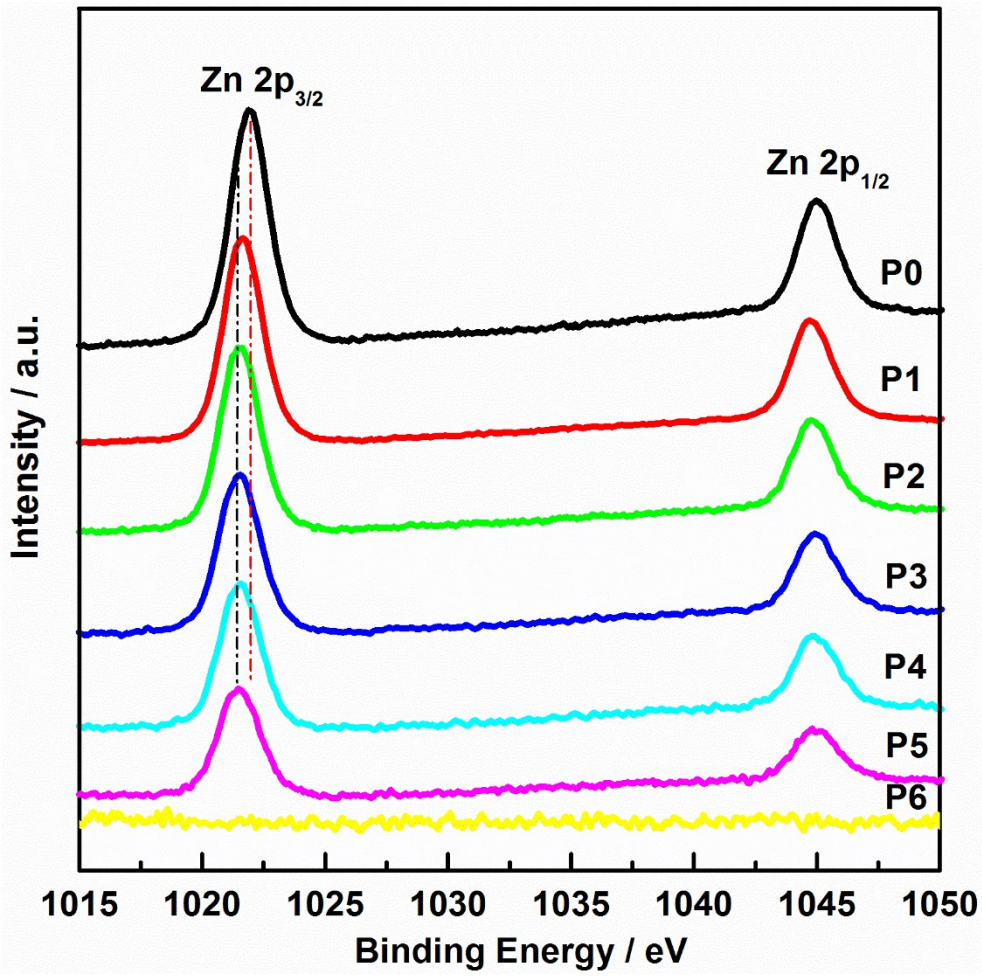

Figure S8. Zn 2p XPS spectra of the P0-P6 sample.

11. LSV of P6 GCE

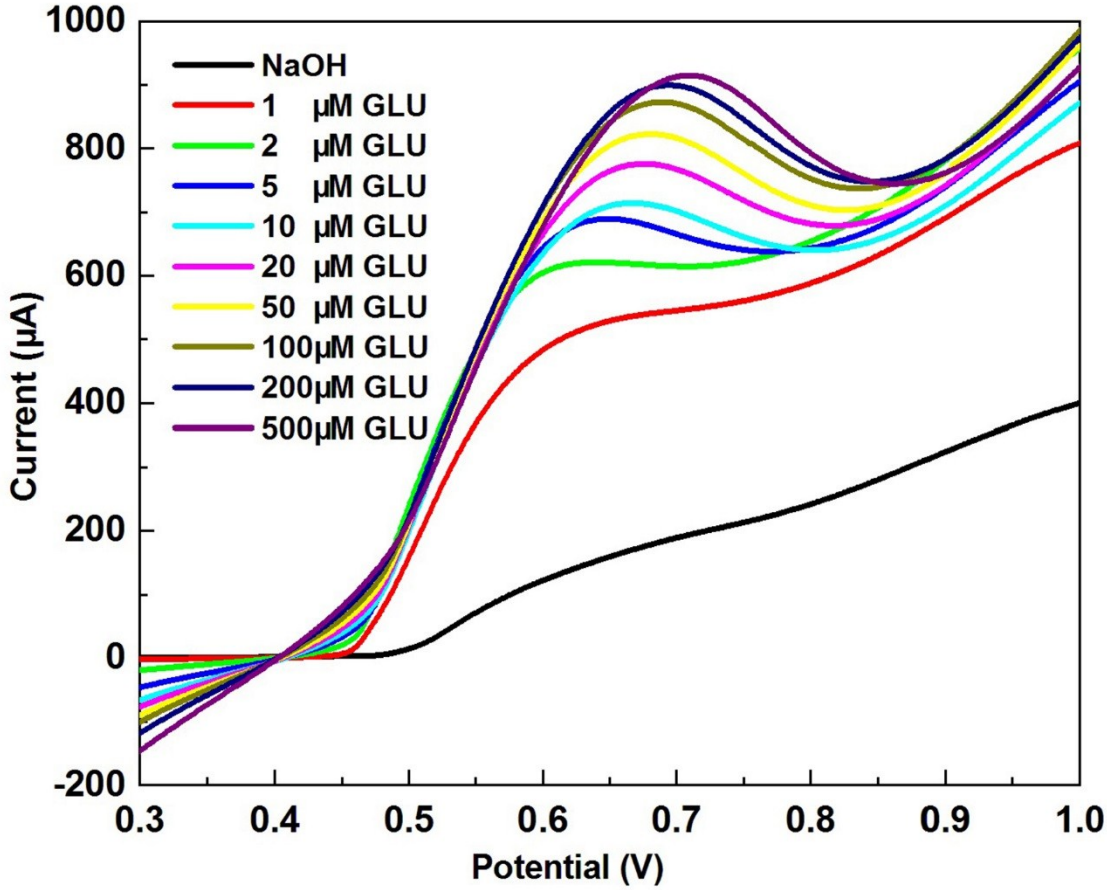

Figure S9. LSVs collected for the P6 GCE with increasing GLU concentration in the range of 1 to 500 μM (scan rate: 100 mV/s).

12. Electrochemical performances of P0 GCE

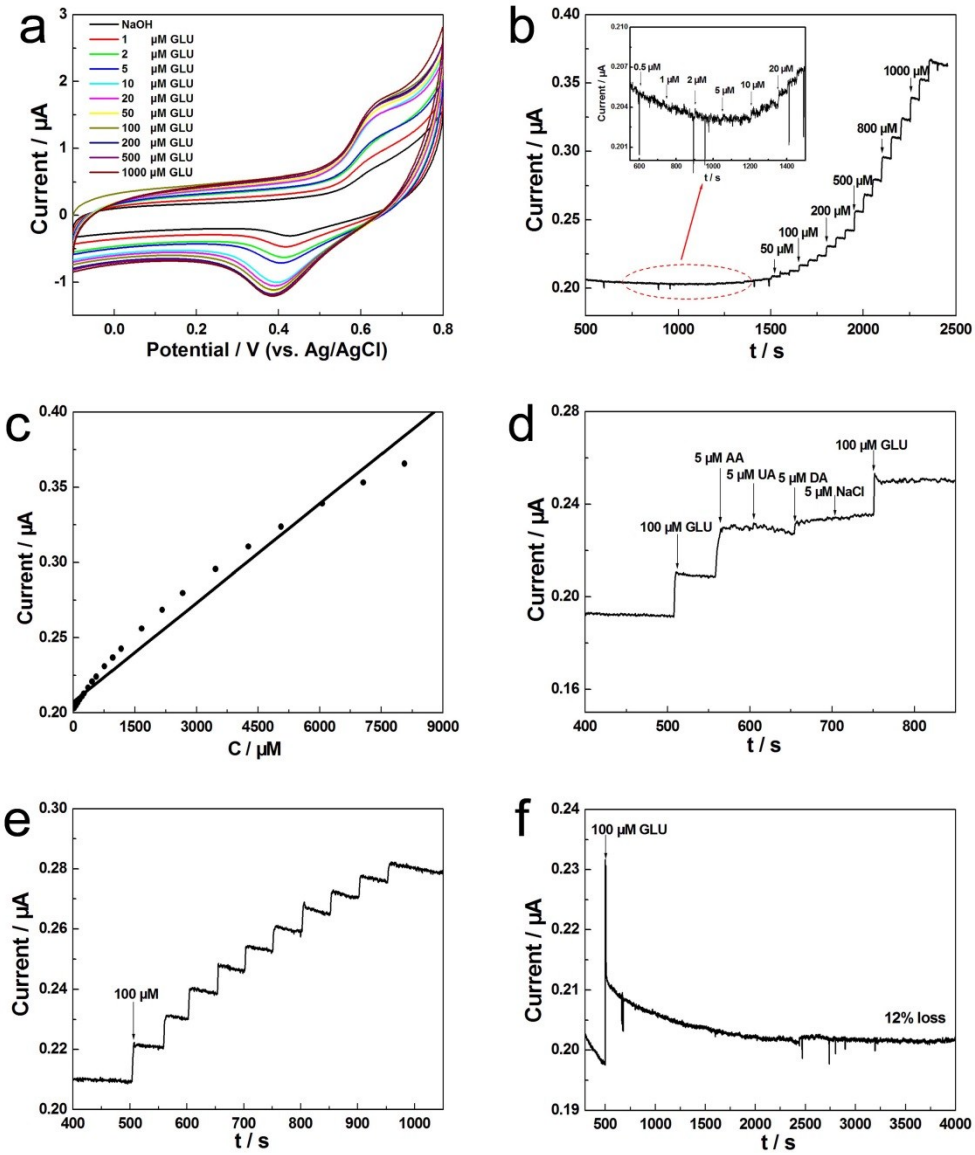

Figure S10. Electrochemical performances of P0 GCE: **(a)** CV curves in NaOH (0.1 M) when adding different concentrations of GLU. **(b)** Current-time response of the P0 GCE at potential of 0.55 V on successive addition of different amounts of GLU in 0.1 M NaOH. **(c)** A plot of electrocatalytic current of GLU vs its concentrations in the range of 0.5 μM to 8.065 mM. **(d)** Current-time response of P0 GCE with addition of 100 μM GLU, 5 μM AA, 5 μM UA, 5 μM DA, 5 μM NaCl, and 100 μM GLU into 0.1 M NaOH at 0.55 V. **(e)** Current-time response of P0 GCE with addition of 100 μM GLU for ten times into 0.1 M NaOH at 0.55 V. **(f)** The stability of the response current for P0 GCE after the addition GLU solution (100 μM) during 4000 s.

13. CV curves of P1-P5 GCE

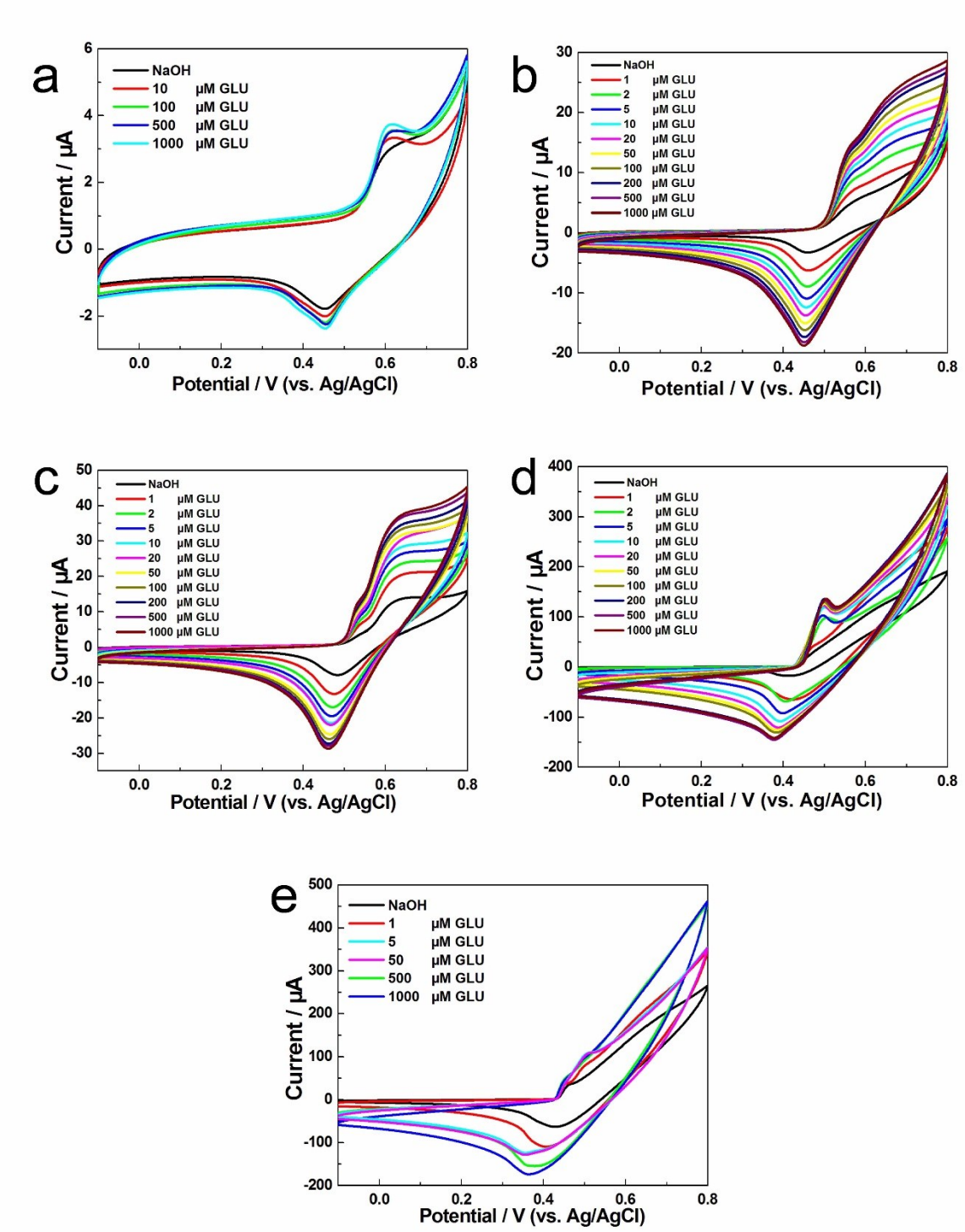

Figure S11. CV curves in NaOH (0.1 M) when adding different concentrations of GLU. (a) P1, (b) P2, (c) P3, (d) P4, (e) P5.

14. Current-time response of P3 GCE at different potentials

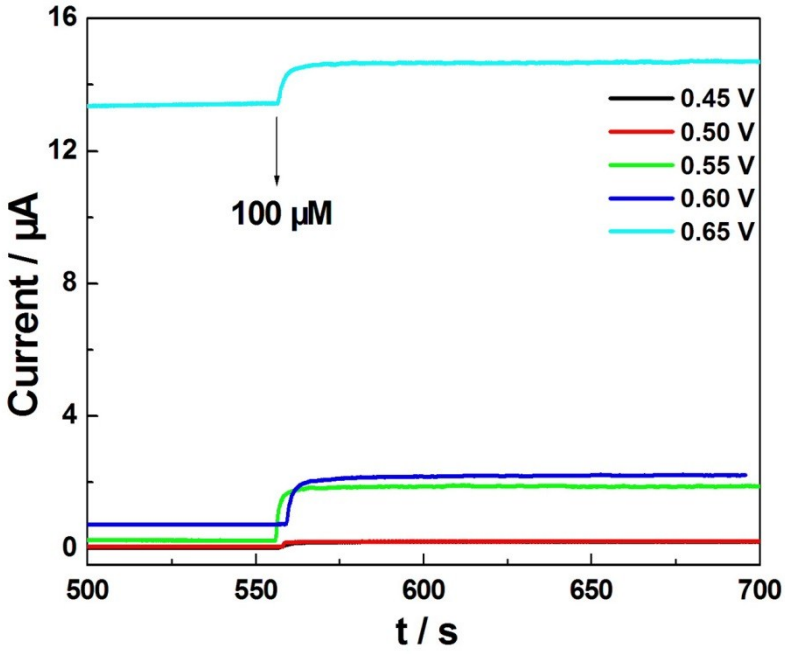

Figure S12. Current-time response of P3 GCE with addition of 100 μM GLU at different potentials of 0.45, 0.50, 0.55, 0.60 and 0.65 V in 0.1 M NaOH.

15. Current-time response of P6 GCE at different potentials

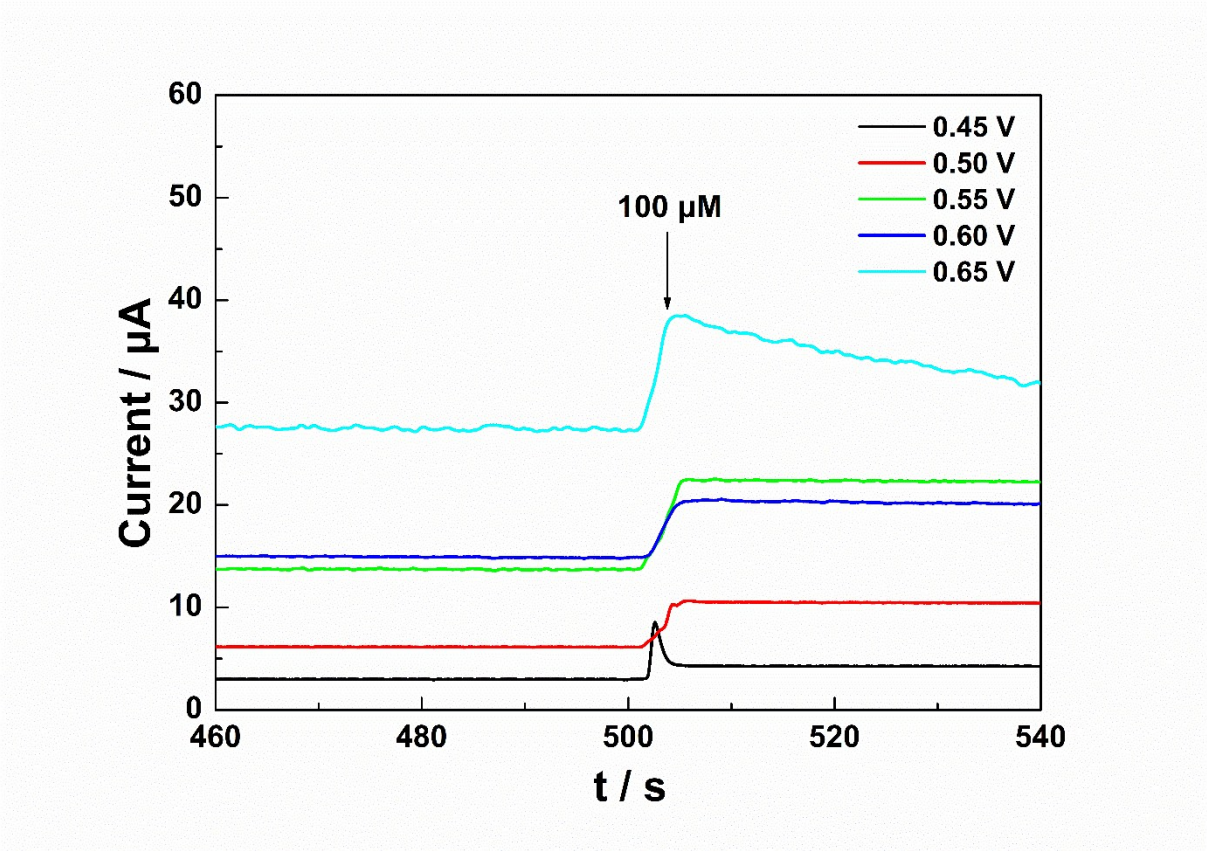

Figure S13. Current-time response of P6 GCE with addition of 100 μM GLU at different potentials of 0.45, 0.50, 0.55, 0.60 and 0.65 V in 0.1 M NaOH.

16. Response time for P6 GCE after the addition glucose solution

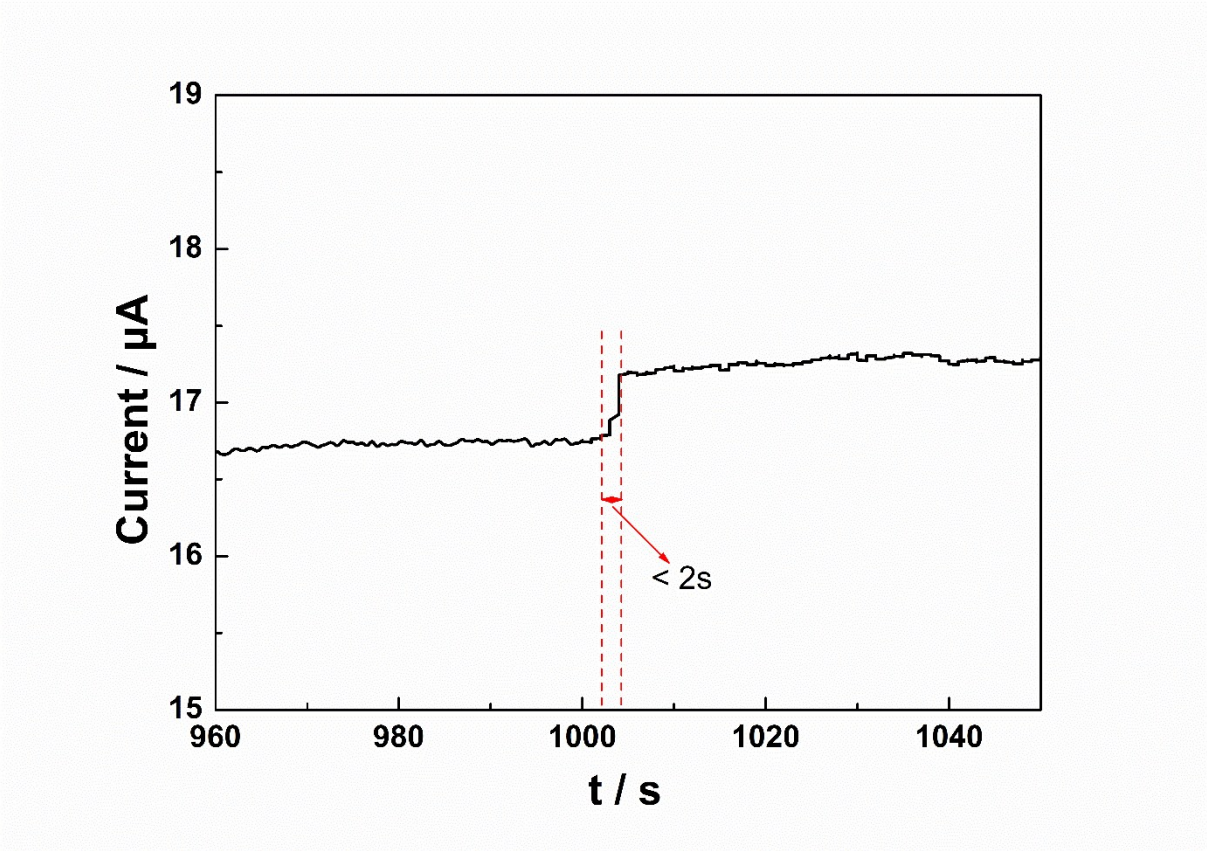

Figure S14. Response time for P6 GCE after the addition glucose solution

17. EIS of P0-P6 GCE

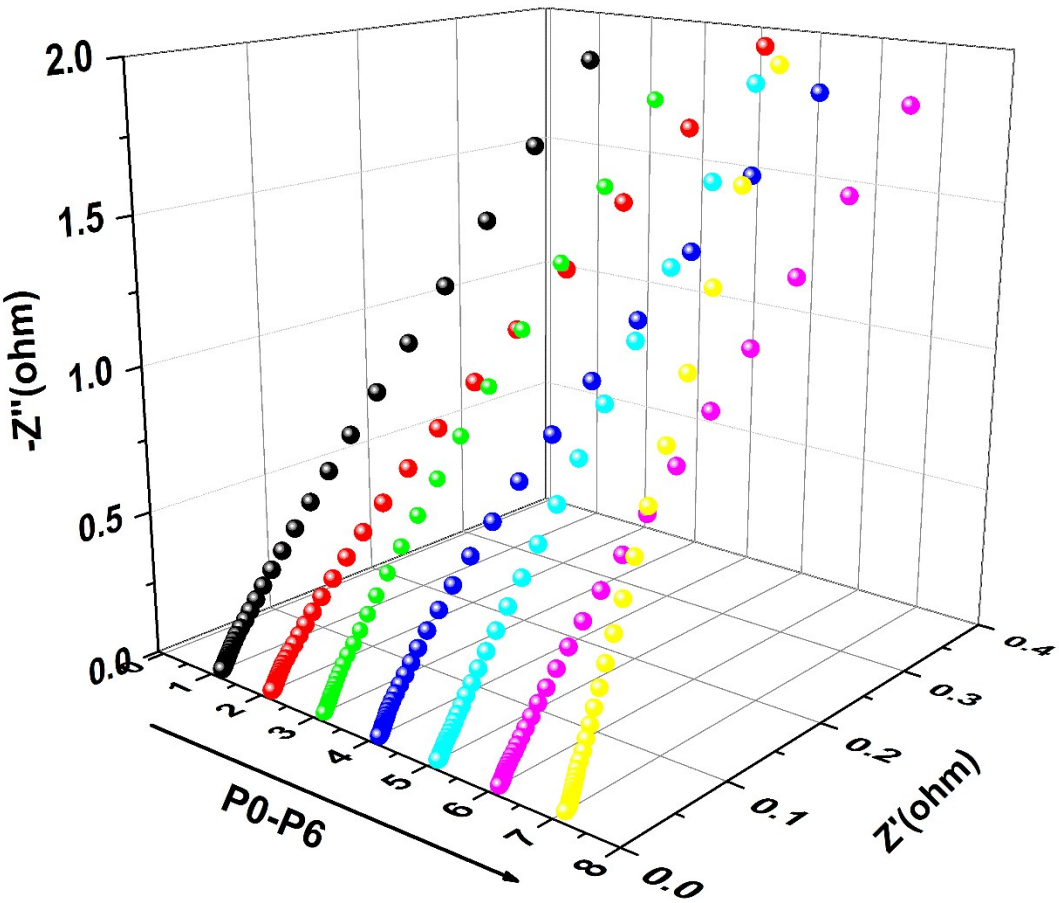

Figure S15. The electrochemical impedance spectra (EIS) of P0-P6 GCE at room temperature is conducted at open circuit voltage in the frequency range of 100 kHZ to 0.01 Hz in 0.1 M NaOH.

18. Molecular structures of P0 and P6

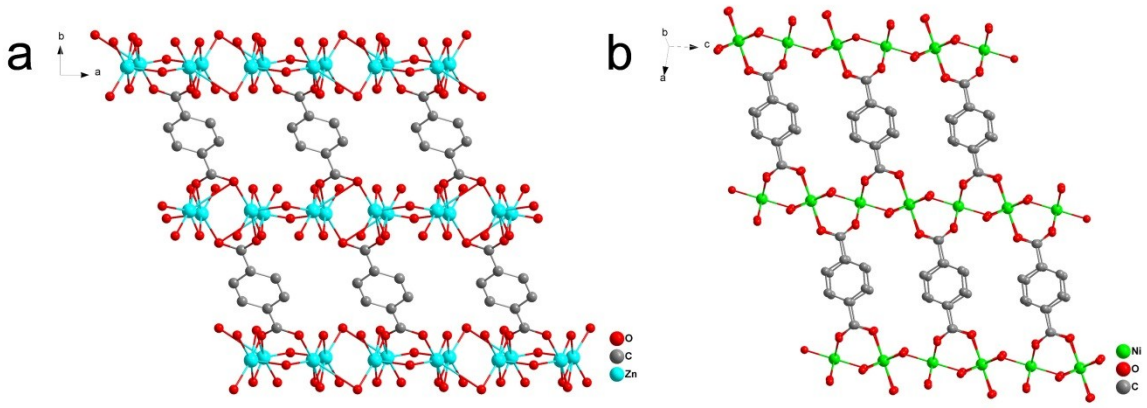

Figure S16. Molecular structures of P0 and P6. (a) P0 and (b) P6.

19. Interlayer distance of P0 and P6

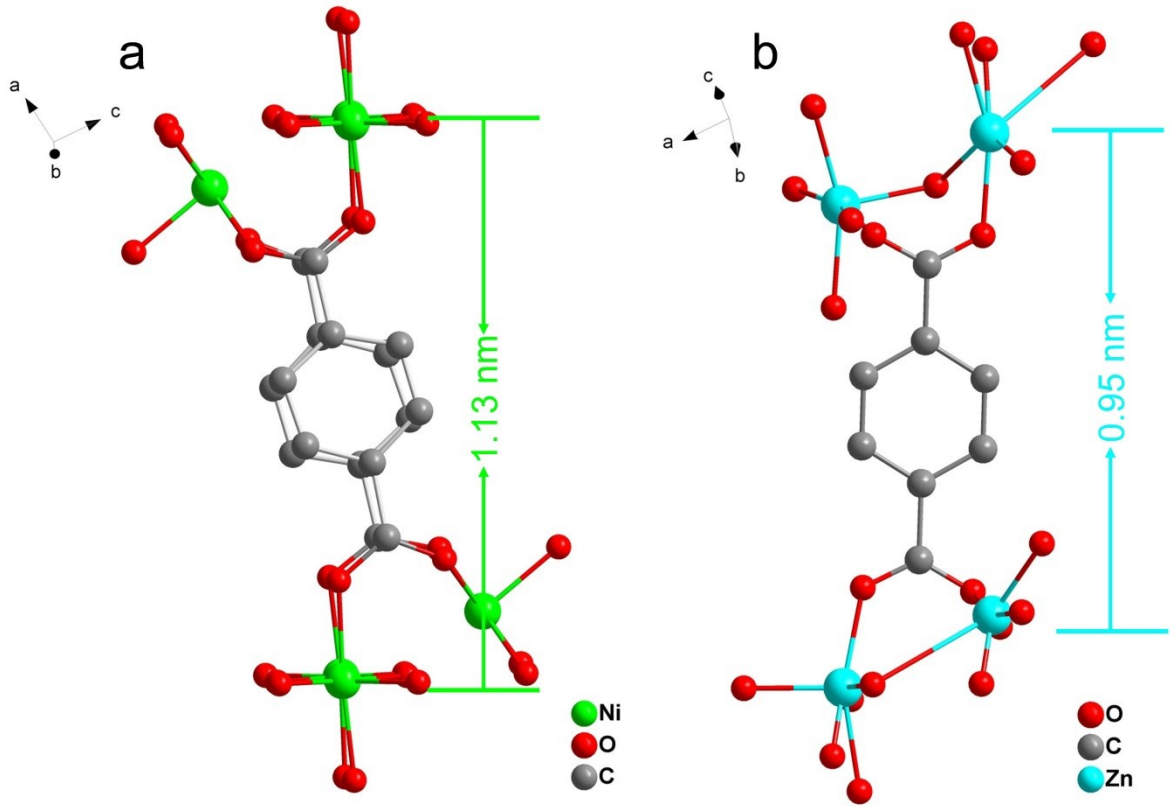

Figure S17. Interlayer distance of P0 and P6. (a) P6 and (b) P0.

20. SEM images of P6 after 48h GOR

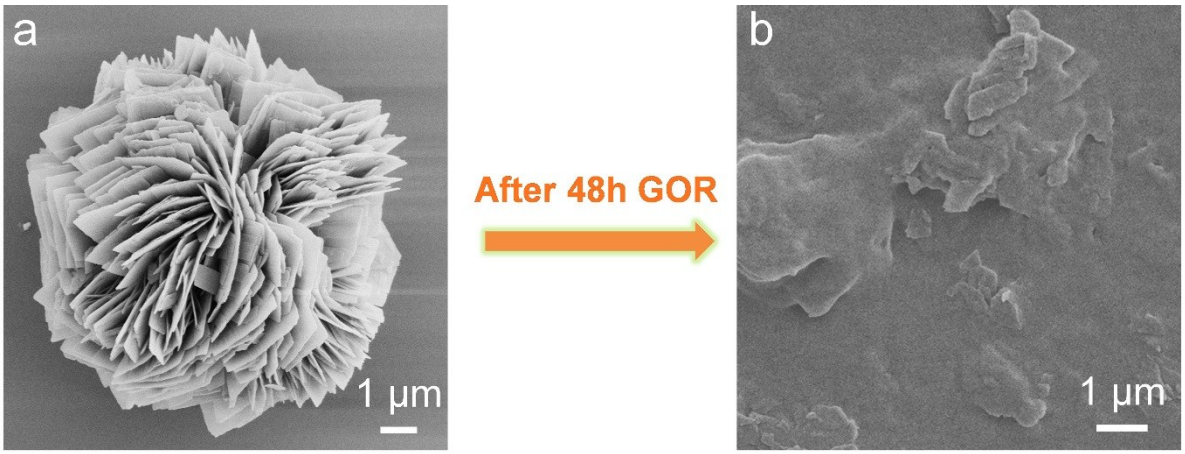

Figure S18. SEM images of: (a) P6 and (b) P6 after 48h GOR.

21. XRD patterns of P6 after 48h GOR

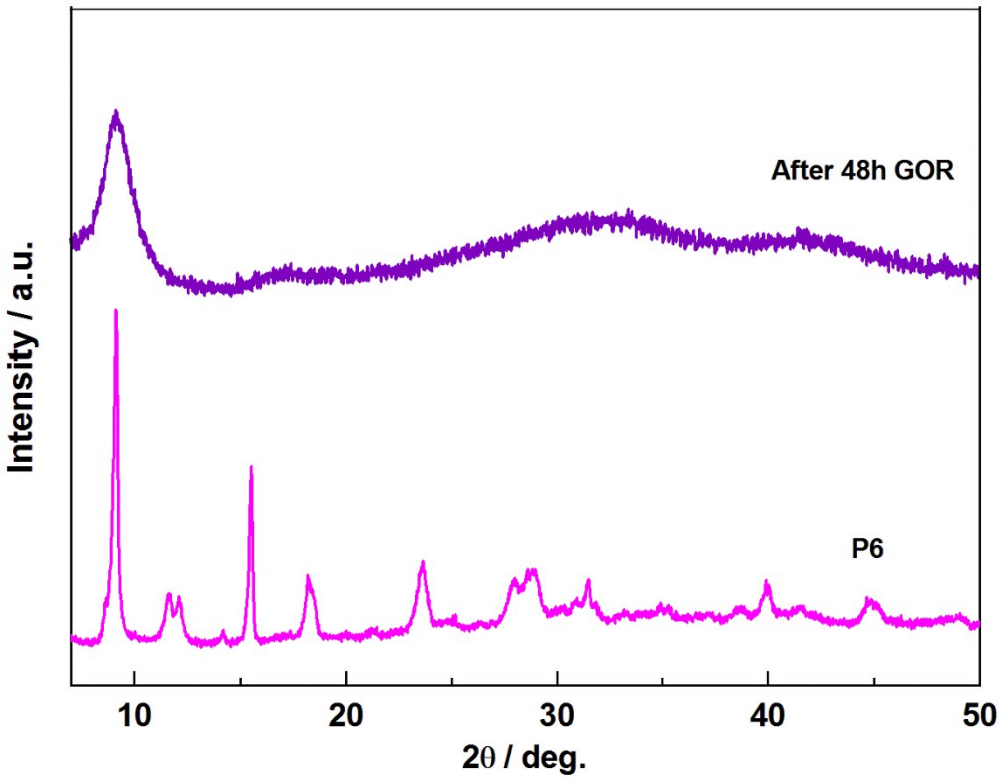

Figure S19. XRD patterns of P6 after 48h GOR.

22. CV curves of P6 after 48h GOR

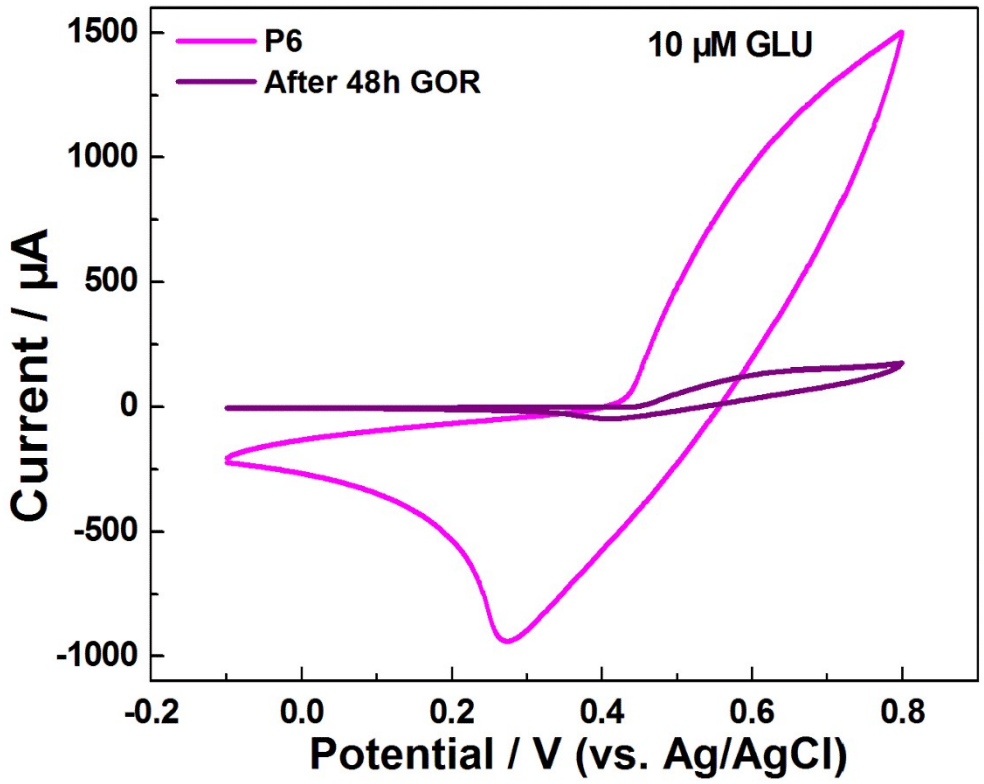

Figure S20. CV curves of P6 and P6 after 48h GOR GCE in NaOH (0.1 M) with 10 μM GLU (scan rate:100 mV·s^{-1}).

23. SEM images of P0/P6

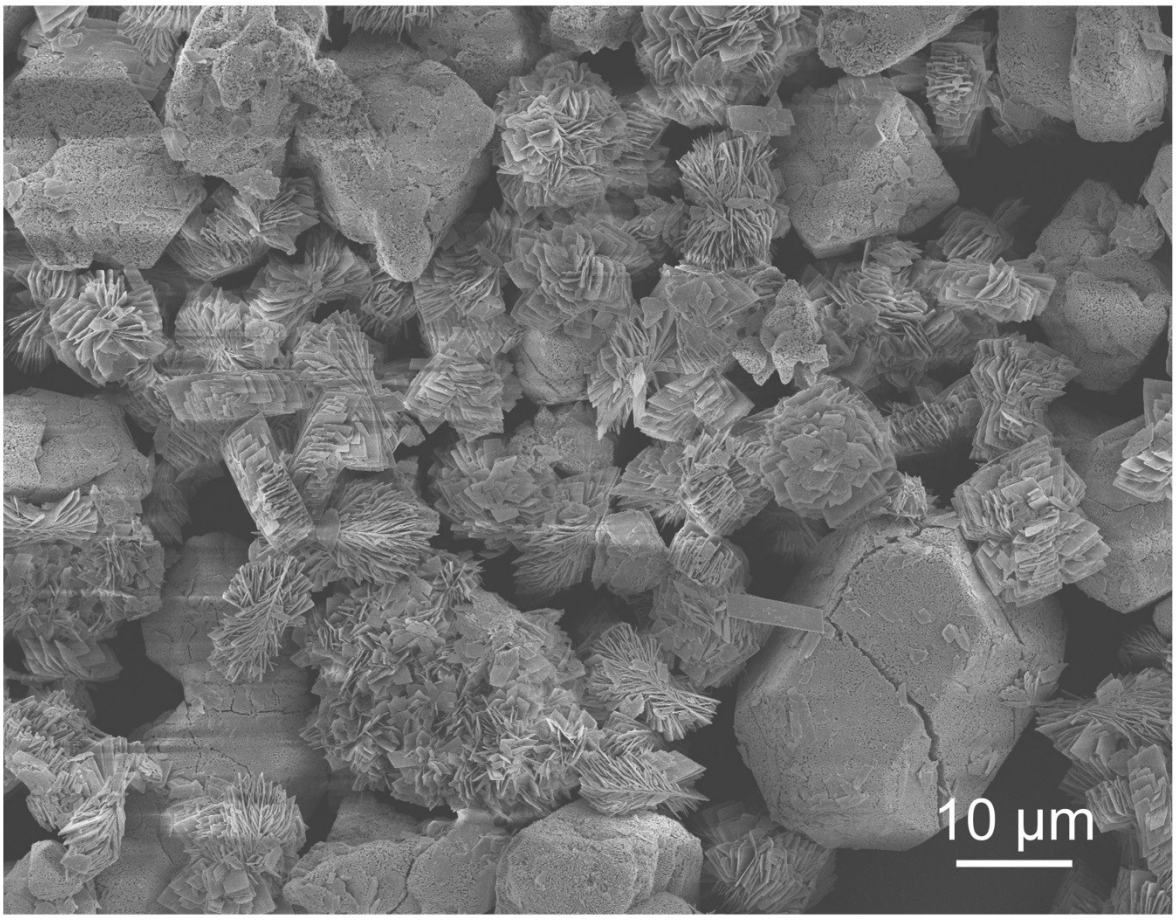

Figure S21. SEM images of P0/P6.

24. XRD patterns of P0/P6

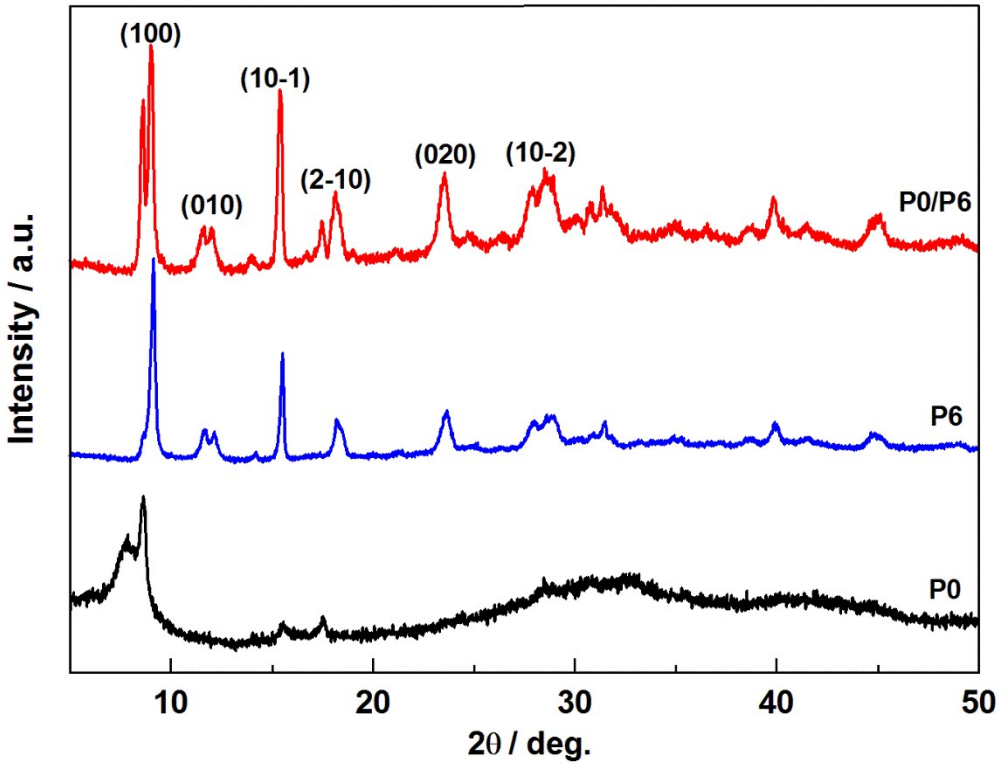

Figure S22. XRD patterns of P0, P6 and P0/P6.

25. CV curves of P0/P6

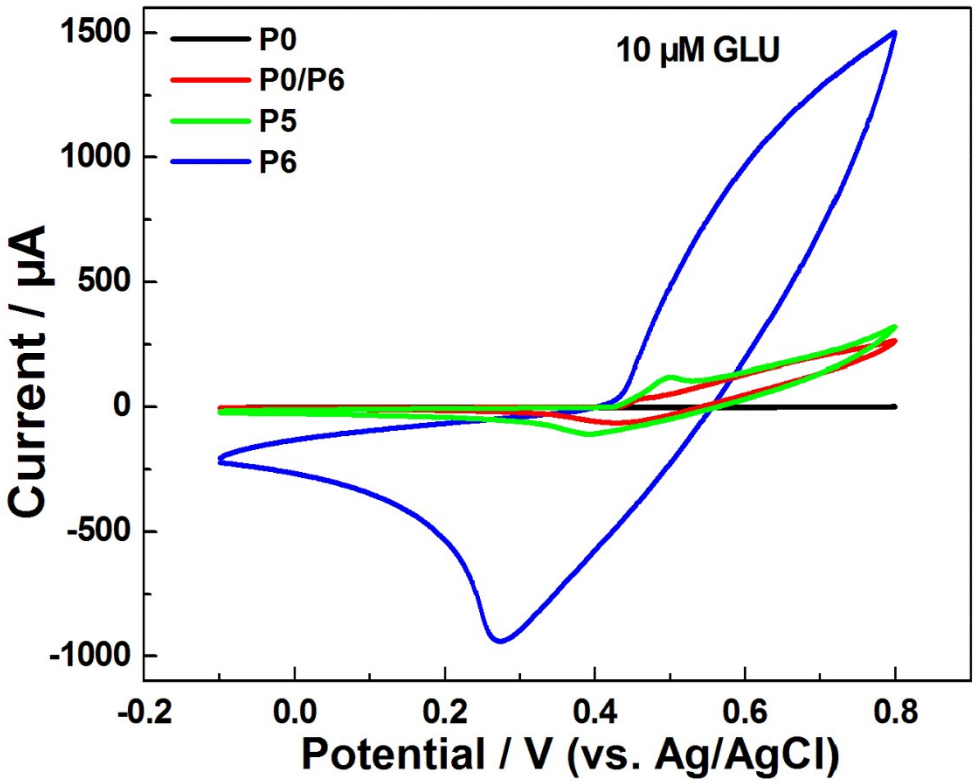

Figure S23. CV curves of P0, P6, P0/P6 and P5 GCE in NaOH (0.1 M) with 10 μM GLU (scan rate:100 mV·s^{-1}).

26. Ni/Zn ratios in mixed-metal MOF samples

Table S1. Ni/Zn ratios in reactants and in mixed-metal MOF samples

MOFs	Ni/Zn ratio in reactants	Ni/Zn ratio in products	
		ICP	EDS
P1(NiZn3-MOF)	1 : 3	1 : 2.96	1 : 2.92
P2(NiZn2-MOF)	1 : 2	1 : 2.01	1 : 1.99
P3(NiZn-MOF)	1 : 1	1.12 : 1	1.19 : 1
P4(Ni2Zn-MOF)	2 : 1	2.02 : 1	1.98 : 1
P5(Ni3Zn-MOF)	3 : 1	3.01 : 1	2.98 : 1

27. Summary of electrochemical performance for as-prepared MOF samples.

Table S2. Summary of electrochemical performance for as-prepared MOF samples.

MOFs	Detection limit (μM)	Linear range (μM)	Sensitivity (μA mM^{-1} cm^{-2})	Stability (loss after 4000 s)
P0(Zn-MOF)	8.125	35-5065	0.31	12%
P1(NiZn3-MOF)	0.625	2.5-5065	2.67	8.5%
P2(NiZn2-MOF)	0.625	2.5-5065	8.75	5.3%
P3(NiZn-MOF)	0.125	0.5-5065	30.86	4.7%
P4(Ni2Zn-MOF)	0.125	0.5-5065	247.98	9.5%
P5(Ni3Zn-MOF)	0.125	0.5-5065	512.53	9.0%
P6(Ni-MOF)	0.125	0.5-8065	1192.64	3.5%

28. Comparison with some Ni-based materials from literature

Table S3. Comparison of electrochemical performance of as-prepared Ni-MOF(P6) with some Ni-based materials from literature.

materials	Detection limit (μM)	Linear range (μM)	Sensitivity (μA mM^{-1} cm^{-2})	References
Ni-MOF(P6)	**0.125**	**0.5-8065**	**1192.64**	**This work**
Ni-MOF/Ni/NiO/C	0.8	4-5664	367.45	[1]
$Ni(OH)_2$ nanowires /Ni foam	1	100-6000	1598	[2]
MOF-3/KSC[a]$_{550}$	4.12	13-4860	448.6	[3]
PDA[b]/ZIF-8@rGO[c]	0.33	1-3600	—	[4]
NiO Superstructures/Foam Ni	6.15	18-1200	395	[5]
rGO[c]/$Ni(OH)_2$ (electrophoretic)	15	0.02-30 mM	1140	[6]
NiCPNP[d]/rGO[c]	0.14	10-8750	—	[7]
$Ni(OH)_2$	0.07	0.5-5000	487.3	[8]
Ni-rGO[c]	1	1-110	813	[9]
rGO[c]-$Ni(OH)_2$	0.6	2-3100	11.43	[10]
NiCFP[e]	1	2-2500	420.4	[11]
NiNWAs[f]	0.1	0.5-7000	1043	[12]

a) KSC: kenaf stem carbon. b) PDA: polydopamine. c) rGO: reduced graphene oxide.
d) NiCPNP: Ni(II)-based metal-organic coordination polymer nanoparticle.
e) NiCFP: Ni nanoparticle-loaded carbon nanofiber paste.
f) NiNWAs: Ni nanowire arrays.

29. References

1 Y. Shu, Y. Yan, J. Chen, Q. Xu, H. Pang and X. Hu, *ACS Appl. Mater. Interfaces*, 2017, acsami.7b07501.

2 Q. Xiao, X. Wang and S. Huang, *Mater. Lett.*, 2017, **198**, 19–22.

3 Y. Zhang, L. Wang, J. Yu, H. Yang, G. Pan, L. Miao and Y. Song, *J. Alloys Compd.*, 2017, **698**, 800–806.

4 Y. Wang, C. Hou, Y. Zhang, F. He, M. Liu and X. Li, *J. Mater. Chem. B*, 2016, **4**, 3695–3702.

5 L. Wang, Y. Xie, C. Wei, X. Lu, X. Li and Y. Song, *Electrochim. Acta*, 2015, **174**, 846–852.

6 P. Subramanian, J. Niedziolka-Jonsson, A. Lesniewski, Q. Wang, M. Li, R. Boukherroub and S. Szunerits, *J. Mater. Chem. A*, 2014, **2**, 5525–5533.

7 W. Lu, X. Qin, A. M. Asiri, A. O. Al-Youbi and X. Sun, *Analyst*, 2013, **138**, 429–433.

8 J. Nai, S. Wang, Y. Bai and L. Guo, *Small*, 2013, **9**, 3147–3152.

9 Z. Wang, Y. Hu, W. Yang, M. Zhou and X. Hu, *Sensors*, 2012, **12**, 4860–4869.

10 Y. Zhang, F. Xu, Y. Sun, Y. Shi, Z. Wen and Z. Li, *J. Mater. Chem.*, 2011, **21**, 16949.

11 Y. Liu, H. Teng, H. Hou and T. You, *Biosens. Bioelectron.*, 2009, **24**, 3329–3334.

12 L.-M. Lu, L. Zhang, F.-L. Qu, H.-X. Lu, X.-B. Zhang, Z.-S. Wu, S.-Y. Huan, Q.-A. Wang, G.-L. Shen and R.-Q. Yu, *Biosens. Bioelectron.*, 2009, **25**, 218–223.